

Cite this: DOI: 10.1039/c2lc21091f

www.rsc.org/loc

PAPER

## Optical classification of algae species with a glass lab-on-a-chip

Allison Schaap,<sup>a</sup> Thomas Rohrlack<sup>b</sup> and Yves Bellouard<sup>\*a</sup>

Received 9th November 2011, Accepted 27th January 2012

DOI: 10.1039/c2lc21091f

The identification of submillimetre phytoplankton is important for monitoring environmental and climate changes, as well as evaluating water for health reasons. Current standard methods for phytoplankton species identification require sample collection and *ex situ* analysis, an expensive procedure which prevents the rapid identification of phytoplankton outbreaks. To address this, we use a glass-based microchip with a microchannel and waveguide included on a monolithic substrate, and demonstrate its use for identifying phytoplankton species. The microchannel and the specimens inside it are illuminated by laser light from the curved waveguide as algae-laden water is passed through the channel. The intensity distribution of the light collected from the biochip is monitored with an external photodetector. Here, we demonstrate that the characteristics of the photodiode signal from this simple and robust system can provide significant and useful information as to the contents of the channel. Specifically, we show first that the signals are correlated to the size of algae cells. Using a pattern-matching neural network, we demonstrate the successful classification of five algae species with an average 78% positive identification rate. Furthermore, as a proof-of-concept for field-operation, we show that the chip can be used to distinguish between detritus in field-collected water and the toxin-producing cyanobacterium *Cyanothece*.

### Introduction

As primary producers of oxygen, phytoplankton are vital to the earth and the identification of microscopic phytoplankton is important for a wide variety of environmental monitoring applications. While thousands of species exist over a wide range of environmental conditions, a given area is often dominated by several species, which can vary according to the local environmental conditions, the time of year, and by human interventions, both deliberate and unintentional. The dynamics of the species populations in a given body of water is thus a useful biomarker for changes occurring in the water and surrounding area.<sup>1</sup> In addition to environmental monitoring, the examination of species is a public health issue: some algae and cyanobacteria produce toxins known to cause negative health effects to animals and humans, including cancer, liver failure, and death.<sup>1-4</sup>

The continued demand for low-cost, portable, robust algae monitoring is driven by several factors, including increased public and governmental attention on algae-related health and safety problems and on climate concerns. For example, regulations introduced by the European Union require the monitoring of the ecological status and bathing (recreational) water quality of lakes using, for example, cyanobacteria and algae as markers.<sup>5</sup> Additionally, the identification of algal species is required for

applications such as the analysis of ballast water<sup>6</sup> and in the development of biofuels based on algal biomass.<sup>7,8</sup>

We present an optofluidic chip-based approach to algae species identification. The device is based on a laser-modified piece of monolithic glass, which provides a robust and low-cost system for particle and algae identification. We demonstrate that the signals obtained from algae and particle specimens can be used to determine the size of the specimen, as well as to classify species in a mixture of five algae species and to distinguish the toxin-producing cyanobacterium *Cyanothece* from detritus collected from a field sample, the latter two classifications using neural networks for pattern recognition.

### State of the art

The current gold standard for the identification of microscopic phytoplankton species (hereafter referred to as algae for convenience) is the collection of samples and later *ex situ* manual identification *via* microscopy by highly trained individuals. Various instrumentation approaches have been presented to automate the identification of algae, some *in situ* but most in a laboratory. On the largest scale, oceanographic images taken by satellites can be analysed to identify large algae blooms; other *in situ* approaches typically perform bulk quantification, by measuring the scattering or fluorescence of a volume of water. Laboratory-based analysis of samples often includes a chemical analysis of the pigments found in a sample or a measurement of the optical absorption spectrum of a sample. These approaches

<sup>a</sup>Department of Mechanical Engineering, Eindhoven University of Technology, Postbus 513, 5600MB Eindhoven, The Netherlands. E-mail: y.bellouard@tue.nl; Fax: +31-40-247-2603; Tel: +31-40-247-3715

<sup>b</sup>Norwegian University of Life Sciences UMB, box 5003, 1432 Ås, Norway

can provide very accurate information about the qualitative composition of the sample, but do not quantify the number or size of algae in the sample.

Yentsch *et al.*<sup>9</sup> pioneered the use of flow cytometers in algae species identification, and that technique has been improved upon by many groups through the present using as-purchased or custom-modified flow cytometers, with data often analysed through discriminant analysis<sup>10,11</sup> or neural networks.<sup>12,13</sup> The move to *in situ* real-time monitoring has been made by a few companies, such as CytoBuoy.<sup>14,15</sup>

With the development of integrated microfluidic lab-on-a-chip systems has come progress in the development of microflow cytometers.<sup>16</sup> While the use of these devices for phytoplankton identification remains relatively rare, it has been demonstrated. Benazzi *et al.*<sup>17</sup> presented a microfluidic system with external optics for microflow cytometry and integrated electrodes for impedance spectroscopy measurements. More recently, a microfluidic chip with waveguides inserted to the material as a part of the fabrication process was shown to provide clusters of fluorescence properties by species.<sup>18</sup> Both of these systems demonstrated that two phytoplankton from different phyla and one cyanobacteria had clearly distinct clusters in plots of the measured fluorescence. However, the use of flow cytometric principles requires that any integrated detection system includes multiple robust laser sources, wavelength-selective filters, and sensitive detectors, which make size and cost reduction difficult.

Femtosecond laser fabrication has been demonstrated as a successful means of microchip fabrication in past work including, for example, chips for the observation of living cells,<sup>19</sup> for the detection and counting of cells,<sup>20,21</sup> and for single-cell optical trapping and stretching.<sup>22</sup> We have also previously demonstrated the use of the present chip for particle counting<sup>23</sup> and the simple distinguishing between two algae categories with manually imposed selection criteria.<sup>24</sup> Here we present a more complete study of the abilities of the device, demonstrating that its output signals can be matched to algae cell volume, that it can be used to classify five mixed algae species, and that it can distinguish between field-sampled detritus and lab-cultured algae.

## Materials and methods

### System principle and setup

The system presented consists of a glass chip with a curved waveguide directing light across a microchannel through which algae-laden water flows (Fig. 1). A fiber-injected laser source is coupled into the waveguide, and the light is detected after it exits the waveguide and crosses the channel with an off-chip four-quadrant detector.

Femtosecond laser exposure combined with chemical etching was used to form a 100  $\mu\text{m}$  by 100  $\mu\text{m}$  cross-section microchannel on the surface of the glass and a curved 8  $\mu\text{m}$  by 8  $\mu\text{m}$  waveguide buried 50  $\mu\text{m}$  below the surface. The channel is approximately 4 cm long, and the waveguide's  $\Delta n$  is  $6.5 \times 10^{-3}$ , with a radius of curvature of 18 mm, and the optical loss of the waveguide is approximately 0.4 dB over its length. The waveguide end is located 500  $\mu\text{m}$  from the microchannel, with the

axis of the waveguide perpendicular to that of the microchannel. The distance between the end of the optical waveguide and the channel is enough that the light exciting from the waveguide (NA = 0.12) expands enough to illuminate the entire height of the channel. Further details of the use of femtosecond lasers for fused silica fabrication have been presented previously<sup>25,26</sup> as have details on the fabrication process for this specific chip.<sup>24</sup>

During experiments, a syringe pump moved particle- or algae-laden water through the channel at 0.4  $\mu\text{L min}^{-1}$ . A microscope objective (20 $\times$ ) and a camera were positioned above the channel, so that the particles or algae could later be identified manually and used to verify the accuracy of the classification system. A laser source (1550 nm) was coupled to the waveguide at the edge of the glass piece. The waveguide's size ensures a stable single-mode light intensity profile. The curve prevents uncoupled light from interacting with the photodiode, increasing the signal to noise ratio of the system. The light coming out of the waveguide slowly diverged (the waveguide NA is about 0.12) and illuminated a four-quadrant detector after passing through the microchannel. The photodetector (New Focus model 2903) was configured such that it returns two signals: one, the intensity of the total detected light ( $I_{\text{total}} = A + B + C + D$ , as in Fig. 1) and the other, the difference between the two upstream detectors and the two downstream detectors ( $\Delta X = (A + B) - (C + D)$ , as in Fig. 1). As the sample passed through the channel, the photodetector signal was monitored and triggered the collection and storage of 100 ms of data at 2 kHz from the photodetector any time the  $\Delta X$  signal passed over a user-programmable threshold. Simultaneously, the capture of an image from the camera was triggered. This image is later used for measuring the accuracy of the detection method.

### Strategy for analysis and classification

Data analysis followed several steps: first, the micrograph of the channel and algae for each dataset was examined to manually identify the algae or particle. Second, several features of the total-intensity and differential signals ( $I_{\text{total}}$  and  $\Delta X$  in Fig. 1) were extracted and subsets of these signal features were used to explore the capabilities of the system through various analyses. The first test looked for correlations between the algae or microsphere size and the photodiode signal features. The second was a classification analysis, to group the algae by species using the signals obtained from the device. Lastly, a test of a field-collected sample spiked with cultured algae was analyzed to test the differentiation between the algae and the detritus collected from a local river.

### Signal characterization

To characterize each particle's or algae cell's photodiode signal, four characteristics of the total intensity ( $I_{\text{total}}$ ) and differential ( $\Delta X$ ) signals were found. These characteristics were the maximum value, the minimum value, the summed signal, and the summed rectified signal divided by the maximum value.

In equation form, for the  $\Delta X$  signal, these are

$$\frac{\max(\Delta X)}{\sum(\Delta X)} \quad \frac{\min(\Delta X)}{\sum(\text{abs}(\Delta X))/\max(\Delta X)}$$

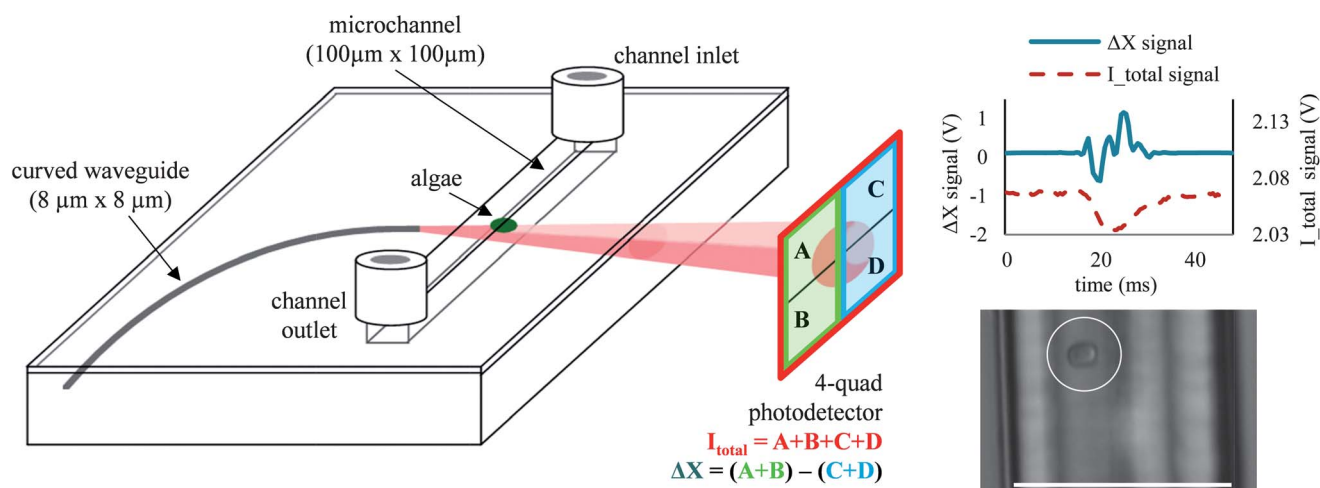


**Fig. 1** (Left) Schematic of the system which features a curved waveguide to direct laser light across a microchannel onto a photodetector; (right) a typical signal obtained, and a photo, triggered by the signal rising above a threshold, of a *Cyanothece* specimen (circled) in the microchannel. The channel width (indicated with the white scale bar) is 100  $\mu\text{m}$ .

### Microsphere and algae size correlations

The literature on algae suggests that knowledge of the size distribution of the algae present in a body of water can be a valuable tool for monitoring the species dynamics.<sup>27</sup> With this motivation, polystyrene microspheres were used to examine the specimen size dependence of the photodetector signals, independent of the varied geometries of the algae. Additionally, nine species of algae were measured and similarly examined (see the Specimens section, below). The total change in the  $I_{\text{total}}$  signal during each passing specimen (that is, the difference between the maximum and the minimum value) was recorded from samples of each size of particle and species of algae.

### Neural network classification

The classification of algae by species, and the differentiation between field samples and lab-cultured algae were performed with a neural network analysis using the pattern recognition feature of the neural network toolbox from the commercially available software MATLAB. In both cases, 10 hidden neurons were used in the network, 70% of the data were used for training for the classification algorithm, and all eight parameters used to characterize the signals obtained from each specimen were used as inputs to the neural network.

### Specimens

Polystyrene microspheres (Corpuscular Inc.) were used for some experiments, to examine the specimen size-dependence of the signal, independent of the varied geometries of the algae. The microspheres had nominal diameters 5  $\mu\text{m}$ , 10  $\mu\text{m}$ , and 20  $\mu\text{m}$ . The spheres were examined by micrograph and a fairly wide distribution of sizes was found; thus in particle size-dependent tests, it was decided to measure the diameter of each individual incident microsphere rather than force a classification into one of the three nominal sizes.

Algae cultures were obtained from the Norwegian Water Research Institute; species, abbreviations, and culture numbers

are listed in Table 1. They were stored in Z8 buffer<sup>28</sup> and diluted with water shortly before use. Micrograph images were used to make measurements of a random selection of 20 cells of each algae species. The volume of each cell was estimated using combinations of simple geometric models—spheres, ellipses, cylinders, and cones—chosen to most closely resemble the cells of each species.

Water was collected from the surface of the slow-moving nearby Dommel River, a tributary of the Maas River, and was used as the basis for the field-sample testing of the device. The river water was passed through a coarse filter to remove material larger than the channel itself, and then lab-cultured *Cyanothece* was added to the river water. After mixing, micrographs of the sample were taken to examine the appearance of the non-*Cyanothece* material in the water (Fig. 6), and then the mixture was passed through the microfluidic channel chip. 106 *Cyanothece* specimen and 216 detritus specimen were manually identified from the simultaneously captured images.

## Results and discussion

Data collected from monocultured algae species (Fig. 2), from the polystyrene microspheres, from the mixture of five algae species, and from the mixture of river-collected detritus and

**Table 1** Algae species

Species name	Short name	Culture number
<i>Cyanothece aeruginosa</i>	S1	NIVA-CYA 258/2
<i>Scenedesmus acuminatus</i>	S2	NIVA-CHL 58
<i>Chlorella vulgaris</i>	S3	NIVA-CHL 19
<i>Microcystis viridis</i>	S4	NIVA-CYA 122/3
<i>Anabaenopsis</i> sp.	S5	NIVA-CYA 417
<i>Navicula pelliculosa</i>	S6	NIVA-BAC 42
<i>Pseudokirchneriella subcapitata</i>	S7	NIVA-CHL 1
<i>Pseudanabaena</i> sp.	S8	NIVA-CYA 504
<i>Monoraphidium griffithii</i>	S9	NIVA-CHL 8

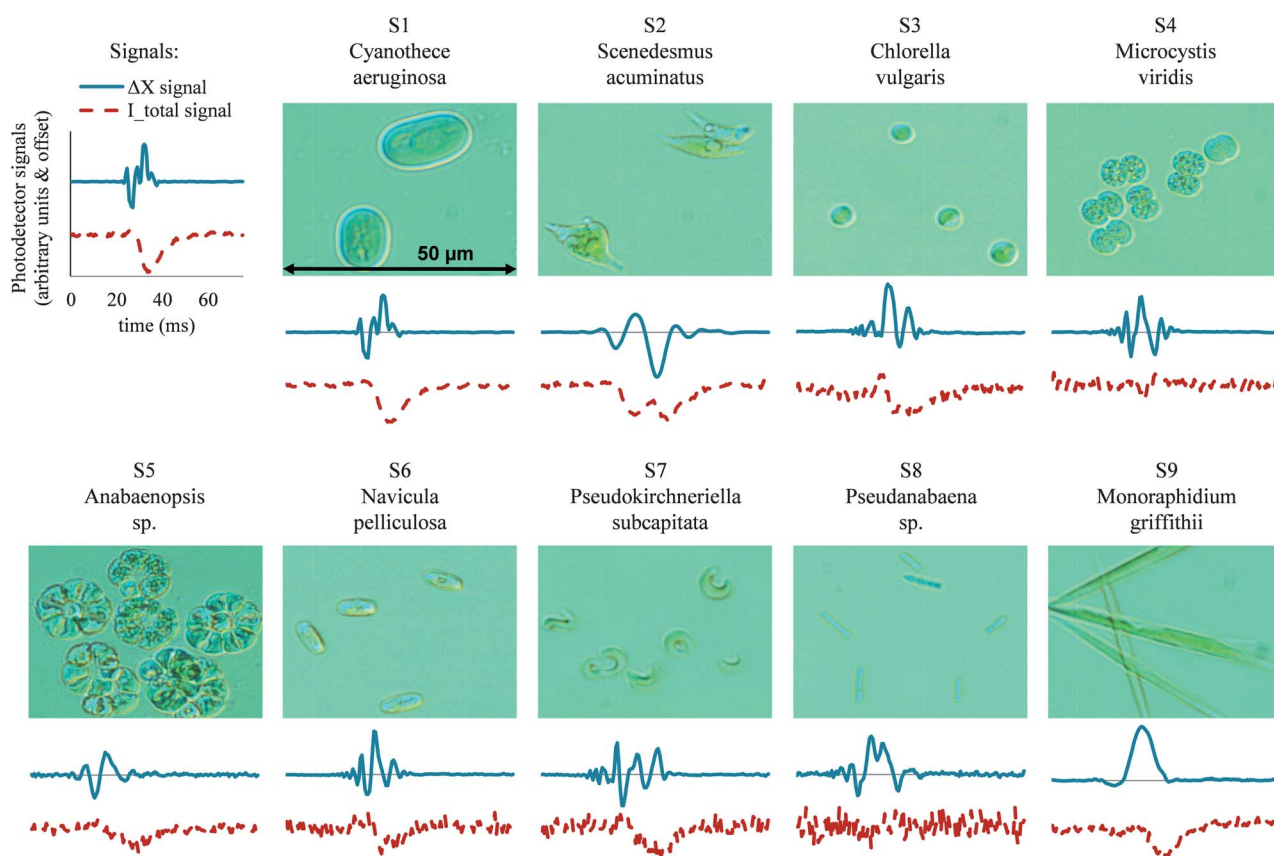


**Fig. 2** Differential ( $\Delta X$ ) and total ( $I_{total}$ ) photodiode signals obtained from nine species of algae, with corresponding micrographs, forming the basis of a library for comparison of data obtained by the optofluidic chip. Data were collected at 2 kHz for 100 ms; 70 ms of data are shown here, with the scaling on the y-axis in arbitrary units.

lab-cultured algae formed the basis for the studies of the chip's capabilities and limitations.

### Microsphere/algae size correlation results

The widespread of the microsphere sizes identified with micrographs motivated a higher resolution of size-classification than the nominal three sizes. The images of the microspheres taken while they were in the channel were processed so that the diameter of each individual sphere could be recorded along with and compared to the photodiode signals. The channel depth was larger than the depth of focus of the microscope objective used to image the channel contents, so the processing step also removed poorly focussed images from consideration, to prevent errors in diameter measurements. After this step, 2994 recorded microsphere datasets remained. The results of the comparison, shown in Fig. 3, are presented with the spheres grouped into integer diameters. The microspheres were tested in a mixture of glycerol and water, to prevent their sinking to the bottom of the channel while in the wide channel entrance area, and the data are thus presented separately, as the index of refraction of glycerol is different from that of water.

Monocultures of algae were run, one species at a time, until at least one thousand instances of each species had been recorded. Within each species, of the images that could be positively

identified as that species, 525 were chosen at random and the photodiode signals compared to the species size. The algae sizes were not measured individually with the in-channel images, but

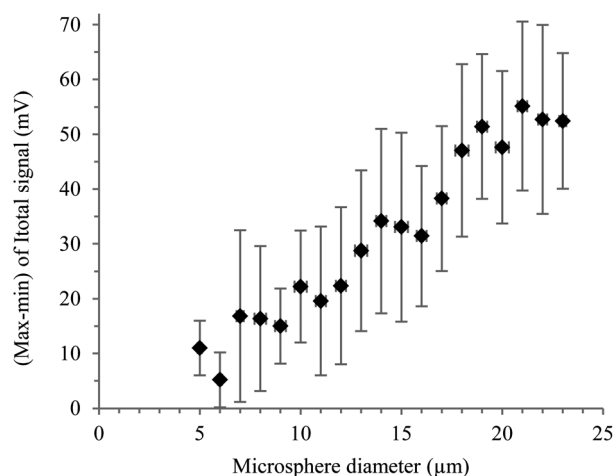


**Fig. 3** The maximum change over time in the total intensity signal from the photodiode was correlated to the average diameter of the microspheres; the diameter of each sphere was measured from the photo of the channel taken simultaneously with the photodiode data and was grouped into the nearest integer diameter. The total number of microspheres was  $N = 2994$ .

those images were used to manually identify the species, and the photodiode signal was compared to the average equivalent diameter of the species.

This approach had to be taken for the algae due to high uncertainties that would be present in the in-channel size measurements. These uncertainties were lower with the microspheres because they were in glycerol, which has an index of refraction closer to that of glass, which led to clearer images.

Both the microsphere and monoculture algae data showed that the average total change in the total intensity photodiode signal  $\max(I_{\text{total}}) - \min(I_{\text{total}})$  closely correlated well with the microsphere diameter or algae equivalent spherical diameters.

### Species classification by neural network

Five species of algae, S1, S3, S4, S5, and S9 (Table 1), were mixed and data collected; the first  $100 \pm 10$  incidences of each species were considered the dataset for classification. All four characteristics of the total intensity ( $I_{\text{total}}$ ) and differential ( $\Delta X$ ) signals—those described above, in “Signal characterization”—were used as inputs to the neural network.

The neural network classifications successfully identified the species of 78% of the algae in the dataset (Fig. 4). The smallest species of the algae samples (*Chlorella vulgaris*, S3, roughly spherical algae with a 6  $\mu\text{m}$  diameter) was the least successfully identified. On the other hand, the larger *Cyanothece* (S1), *Anabaenopsis* (S5), and *Monoraphidium* (S9) were all identified with success rates above the average success rate for the five species. Their equivalent spherical diameters were on average 2.0, 1.7, and 1.4 times larger than S3's, respectively. As can be seen from the algae size data (Fig. 5), the smaller-volume algae had less distinct and species-dependent changes in the photodiode  $I_{\text{total}}$  signal than the larger ones; this could be a contributing factor to the lower success rate in distinguishing the smallest species.

### Distinguishing *Cyanothece* from field-collected detritus

The same neural network classification was applied to data obtained from the mixture of *Cyanothece* and river water

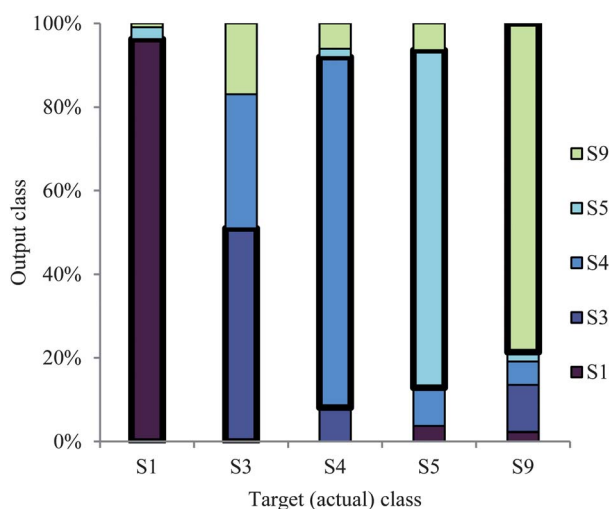


**Fig. 4** Results of neural network classification of five mixed species of algae; species abbreviations are as in Table 1. The correctly identified tests are bordered in a bold line.

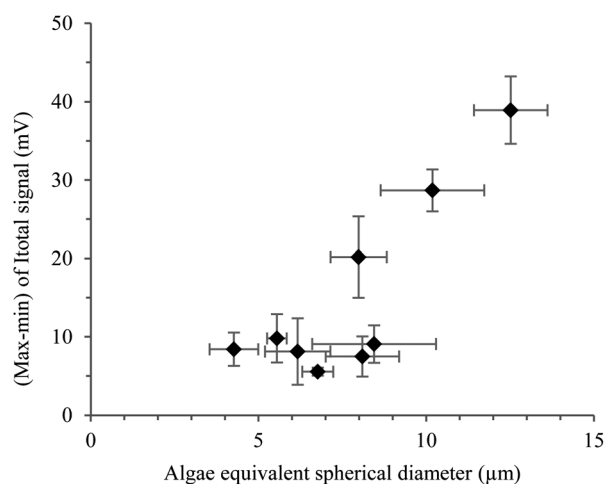


**Fig. 5** The change over time in the total intensity signal from the photodiode was correlated to the average equivalent spherical diameter of the algae cells; the equivalent spherical diameter is a mean of the measurements of twenty micrographs, and the change in total intensity signal is an average of over 525 occurrences of each species.

detritus, to establish a preliminary understanding of how this approach would perform in a field-deployable device.

Of the 106 *Cyanothece*, 100 were correctly classified as *Cyanothece* by the neural network; of the 216 detritus samples, 207 were correctly classified as such. This means that 8% of the samples identified as *Cyanothece* were false positives, while 3% of the samples identified as detritus were false negatives. This high rate of success is likely primarily attributable to the distinct and regular geometry of the *Cyanothece* relative to that of the detritus, which included other algae as well as irregularly shaped matter (Fig. 6).

### Device performance and field deployability

Various aspects of the current device design could be modified to improve performance in a field-deployable system. The two main concerns are those of microchannel clogging and throughput rates.



**Fig. 6** Compounded image of lab-cultured *Cyanothece* (green spheres/ellipses) and amid detritus (other algae, plant matter) from the field-collected sample. The scale bar (bottom of the image) is 100  $\mu\text{m}$ .

The potential for channel clogging would be significant in an uncontrolled, outdoor environment. An ideal system would be able to handle phytoplankton ranging in size from 1  $\mu\text{m}$  up to several hundred micrometres,<sup>29</sup> which could be accomplished by creating multiple parallel sensing channels of different sizes, with a rough size-based pre-sorting step upstream of the sensors. Even so, a pre-filtering system would be necessary to ensure that objects larger than the largest microchannel did not pass into the system. Such a filtration system could use a membrane filter, which has the disadvantage of becoming clogged with time, potentially affecting the device's pressure and flow rate characteristics and eventually needing cleaning or replacement. An alternative, particularly at high flow rates, might be a flow-dynamics-based method, such as the virtual impactors used to remove large airborne particles from aerosol samplers.

To sample as much water as possible, the device throughput rate would need to be increased as much as possible without loss of information. As it is used currently, the device's flow rate is limited by the need to take clear photos of the algae in the microchannel for separate, manual identification to confirm the device performance. Without this limitation, the flow rate could be significantly increased, as long as the collection rate of the photodiode data increased correspondingly. Even with the photodiode and data acquisition system presently used, the data collection rate could be increased at least 20-fold if the *in situ* images were not collected. The other aspect to throughput rate—that of data analysis—would depend on the eventual system. Portable systems with pre-defined neural networks implemented on microcontrollers have been demonstrated for other applications.<sup>30</sup>

## Conclusions

This simple, robust, monolithic optofluidic chip with a microchannel and integrated, sub-surface curved waveguide yields data suitable for the classification of microspheres and algae. It has been shown to provide size-sensitive information, as well as to provide sufficient information for the classification of five different algae species with 78% accuracy. The monolithic nature of the chip renders it less susceptible to mechanical failure than multi-component devices. Its promise as a field-deployable device was demonstrated by a success rate of over 90% in distinguishing between cyanobacteria and field-collected detritus.

Our system offers several advantages to the existing technology in microfluidic-based algae detection. The ability to write three-dimensional waveguides into the bulk of the material removes the issues of aligning external optics or of inserting optical fibres into the system as a fabrication step, making the device more robust. Furthermore, the detection approach—that of a single laser source illuminating a single detector—is simple and requires a minimum number of components, and yet provides enough data to yield successful and useful results for the measurement and classification of algal cells.

## Acknowledgements

The authors would like to acknowledge Translume, Inc. for the microchip fabrication and the Norwegian Water Research Institute for providing the algae cultures. This work is partially

supported by the 7<sup>th</sup> Framework Programme of the European Commission ('Femtoprint', <http://www.femtoprint.eu>).

## Notes and references

- 1 L. Barsanti and P. Gualtieri, *Algae: Anatomy, Biochemistry, and Biotechnology*, CRC Press, 1st edn, 2005.
- 2 E. M. Jochimsen, W. W. Carmichael, J. S. An, D. M. Cardo, S. T. Cookson, C. E. Holmes, M. B. Antunes, D. A. de Melo Filho, T. M. Lyra, V. S. Barreto, S. M. Azevedo and W. R. Jarvis, *N. Engl. J. Med.*, 1998, **338**, 873–878.
- 3 L. Zhou, H. Yu and K. Chen, *Biomed. Environ. Sci.*, 2002, **15**, 166–171.
- 4 I. Chorus and J. Bartram, *Toxic Cyanobacteria in Water: a Guide to Their Public Health Consequences, Monitoring and Management: a Guide to Public Health Consequences and Their Management in Water Resources and Their Supplies*, Taylor & Francis, 1st edn, 1999.
- 5 European Parliament, Directive 2006/7/EC of the European Parliament and of the Council of 15 February 2006 concerning the management of bathing water quality and repealing Directive 76/160/EEC, *Off. J. Eur. Communities: Legis.*, 2006, **49**, 37.
- 6 G. M. Ruiz, T. K. Rawlings, F. C. Dobbs, L. A. Drake, T. Mullady, A. Huq and R. R. Colwell, *Nature*, 2000, **408**, 49–50.
- 7 L. Brennan and P. Owende, *Renewable Sustainable Energy Rev.*, 2010, **14**, 557–577.
- 8 T. M. Mata, A. A. Martins and N. S. Caetano, *Renewable Sustainable Energy Rev.*, 2010, **14**, 217–232.
- 9 C. M. Yentsch, P. K. Horan, K. Muirhead, Q. Dortch, E. Haugen, L. Legendre, L. S. Murphy, M. J. Perry, D. A. Phinney, S. A. Pomponi, R. W. Spinrad, M. Wood, C. S. Yentsch and B. J. Zahuranec, *Limnol. Oceanogr.*, 1983, **28**, 1275–1280.
- 10 A. Becker, A. Meister and C. Wilhelm, *Cytometry*, 2002, **48**, 45–57.
- 11 M. R. Carr, G. A. Tarran and P. H. Burkill, *J. Plankton Res.*, 1996, **18**, 1225–1238.
- 12 L. Boddy, C. Morris, M. Wilkins, L. Al-Haddad, G. Tarran, R. Jonker and P. Burkill, *Mar. Ecol.: Prog. Ser.*, 2000, **195**, 47–59.
- 13 H. W. Balfourt, J. Snoek, J. R. M. Smiths, L. W. Breedveld, J. W. Hofstraat and J. Ringelberg, *J. Plankton Res.*, 1992, **14**, 575–589.
- 14 J. C. H. Peeters, G. B. J. Dubelaar, J. Ringelberg and J. W. M. Visser, *Cytometry*, 1989, **10**, 522–528.
- 15 G. B. J. Dubelaar, A. C. Groenewegen, W. Stokdijk, G. J. Van Den Engh and J. W. M. Visser, *Cytometry*, 1989, **10**, 529–539.
- 16 J. Godin, C.-H. Chen, S. H. Cho, W. Qiao, F. Tsai and Y.-H. Lo, *J. Biophotonics*, 2008, **1**, 355–376.
- 17 G. Benazzi, D. Holmes, T. Sun, M. C. Mowlem and H. Morgan, *IET Nanobiotechnol.*, 2007, **1**, 94.
- 18 N. Hashemi, J. S. Erickson, J. P. Golden, K. M. Jackson and F. S. Ligler, *Biosens. Bioelectron.*, 2011, **26**, 4263–4269.
- 19 Y. Hanada, K. Sugioka, H. Kawano, I. S. Ishikawa, A. Miyawaki and K. Midorikawa, *Biomed. Microdevices*, 2007, **10**, 403–410.
- 20 M. Kim, D. J. Hwang, H. Jeon, K. Hiromatsu and C. P. Grigoropoulos, *Lab Chip*, 2009, **9**, 311–318.
- 21 D. N. Schafer, E. A. Gibson, E. A. Salim, A. E. Palmer, R. Jimenez and J. Squier, *Opt. Express*, 2009, **17**, 6068–6073.
- 22 N. Bellini, K. C. Vishnubhatla, F. Bragheri, L. Ferrara, P. Minzioni, R. Ramponi, I. Cristiani and R. Osellame, *Opt. Express*, 2010, **18**, 4679–4688.
- 23 V. K. Pahlwani, Y. Bellouard, A. A. Said, M. Dugan and P. Bado, *Proc. SPIE*, 2007, **6715**, 67150H.
- 24 A. Schaap, Y. Bellouard and T. Rohrlack, *Biomed. Opt. Express*, 2011, **2**, 658–664.
- 25 Y. Bellouard, A. Said and P. Bado, *Opt. Express*, 2005, **13**, 6635–6644.
- 26 Y. Bellouard, A. Said, M. Dugan and P. Bado, *Opt. Express*, 2004, **12**, 2120–2129.
- 27 E. Marquis, N. Niquil and C. Dupuy, *J. Plankton Res.*, 2011, **33**, 1104–1118.
- 28 Scandinavian Culture Collection of Algae & Protozoa, "Z8", <http://www.sccap.dk/media/freshwater/7.asp>.
- 29 J. S. Erickson, N. Hashemi, J. M. Sullivan, A. D. Weidemann and F. S. Ligler, *Anal. Chem.*, 2012, **84**, 839–850.
- 30 E. Garcia-Breijo, J. Atkinson, L. Gil-Sanchez, R. Masot, J. Ibanez, J. Garrigues, M. Glanc, N. Laguarda-Miro and C. Olguin, *Sens. Actuators, A*, 2011, **172**, 570–582.